Pulse-level Beam-switching MAC with Energy Control in Picocell Terahertz Networks

Jian Lin and Mary Ann Weitnauer
School of Electrical and Computer Engineering
Georgia Institute of Technology, Atlanta, Georgia 30332–0250
Email: jlin61@gatech.edu; maweit@gatech.edu

***Abstract*—Terahertz Band (0.1-10 THz) wireless communication, which escalates the frequency and provides unprecedented data rates, is envisioned as the key picocell wireless technology in the next five to ten years. In this band, the medium access control (MAC) is more about "scheduling transmissions," instead of "fighting for access," thanks to the huge bandwidth. On the one hand, an electronically steerable narrow beam is essential to overcome the high path loss at THz and extend the communication range. On the other hand, impulse radio in THz Band that generates femtosecond-long pulses enables the beam direction to be switched at the "pulse-level," in contrast to the conventional "packet-level" switching as seen in literature. To capture these features, yet keep complexity low, we assume a simple time-spread on-off-keying (TS-OOK) emitter and energy detection receiver. In this paper, we present the first MAC design to enable macro-scale communication at 100 Gbps by exploring THz Pulse-level Beam-switching with Energy control (TRPLE). For the downlink, the data rate of an arbitrary user and the network throughput are analytically investigated.**

***Index Terms*—Terahertz Band, Beamsteering, MAC, Ultra-broadband communication**

I. Introduction

Wireless data traffic has drastically increased accompanied by an increasing demand for higher speed wireless transmission. In particular, wireless data rates have doubled every 18 months over the last three decades and are quickly approaching the capacity of wired communication systems according to Edholm's law of bandwith [1]. Following this trend, Terabit-per-second (Tbps) short-range communication in the Terahertz (THz) Band (0.1-10 THz) is envisioned as a key wireless technology in the next decade [2] [3] [4] [5]. Enabling THz Band communication will address the spectrum scarcity and capacity limitations of current cellular system, and will boost a plethora of applications in biomedical, environmental, industrial and military fields [2] [3]. Though much research has been recently performed towards channel modeling, antenna design and transceiver design [3], the protocol design in the system level is still unsolved. Also, existing research mainly focuses on nano-scale applications [6]. In this paper, we propose the first MAC protocol that is suitable for THz Band communication in the indoor picocell.

The peculiarities of the THz Band limit its range, compared to 60 GHz or ultra-wideband (UWB), and distinguish THz from conventional wireless systems. According to the channel model [7], Fig.1 depicts the overall path loss in the THz Band plotted linearly over frequencies and logarithmically over distances. The path loss consists of spreading loss and molecular absorption loss. The spreading loss accounts for the attenuation due to the expansion of the wave as it propagates in the medium. The absorption loss accounts for the conversion of wave energy to kinetic energy in various molecules (predominantly H_2O) and thus makes THz channel strongly frequency-selective and lossy. While large distances (km) exhibit very high path loss, the short ranges (mm) see the entire THz Band as a single transmission window due to negligible molecular absorption, which greatly simplifies system design. More interesting observations can be made in the macro-scale (m). From Fig.1, contrary to classical wireless networks, molecular absorption defines multiple transmission windows, which are each several tens of Gigahertz wide and which support the transmission at very high bit-rates; second, the bandwidth of each window is not a fixed value, but there is a unique dependence between the transmission distance, the 3dB bandwidth of each transmission window and the achievable bit rate.

To overcome the extensive transmission loss, it is essential to utilize very large antenna arrays with electronic beam-steering capability [3]. However, the study of directional networking must be distinguished from the existing designs for cellular [8], broad-band [9], and WIFI based multihop wireless networks [10] operating at lower radio frequency (RF) bands, for the following reasons. First, the fact that the directivity achieved in THz Band is much higher gives a "pseudo-wired" abstraction of the wireless link and switches the role of the MAC to "coordination and scheduling" from the conventional "fighting for access." Second, most of existing protocols reply on omni-directional or sector-directional mode to solve neighbor discovery or the deafness problem. This dual-mode is not appropriate for THz because fully directional transmission is required to simply achieve the desired distance. For example, the only existing MAC protocol PHLAME [11] designed for nano-network operating in Terahertz can work only in micro-scale, because PHLAME is in the "omni" catergory. Third, direct paths could be completely blocked by obstacles between a transmitter and its receiver. The blockage foresees and necessitates directed non-line-of-sight (NLOS) paths reflected from walls, ceilings or a dedicated reflective

*Mary Ann Weitnauer was formerly Mary Ann Ingram. The authors gratefully acknowledge support for this research from the U.S. National Science Foundation (NSF) under grant No. CCF-1349828.

978-1-4799-3512-3/14/$31.00 ©2014 IEEE

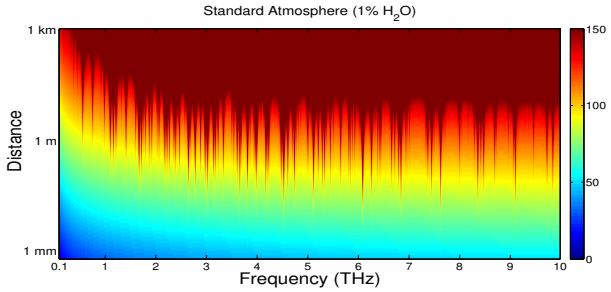

Figure 1: Path loss (in dB) in THz Band v.s. distances and frequencies. The peaks are caused by molecular absorption.

mirror [3], requiring new MAC solutions.

In this paper, targeting the macro-scale communication in the order of meters, we present the system design and numerical analysis for a fully directional MAC for THz networks that relies on pulse-level beam-switching and pulse repetition for energy control (TRPLE). Our approach is motivated by the advancements in Graphene-based electronics, including the novel plasmonic nano-antennas [12], compact plasmonic pulse generators and detectors [13] [14], and nano-antenna arrays with scanning capability [15]. On the other hand, the feasibility of carrier-based modulation is limited by the lack of compact transceivers able to generate carriers at THz Band frequencies. Recently, femtosecond-long pulse-based modulation has been proposed to capture the expected capabilities of THz signal generator and detectors [16]. However, for the time being, pulse-based directional transmission has not been explored in system design in THz networks. Aimed to fill this gap, this paper presents the MAC design to capture the peculiarity of THz channel and the expected THz transceiver capabilities, as well as analytical studies to quantify the system capacity at macro-scale ranges.

The rest of the paper is organized as follows. Section II describes the assumptions on the modulation scheme and device capability. Section III presents the details of TRPLE MAC protocol that solves the neighbor discovery, transmission scheduling, and energy control. Analytical investigations for single user data rate and network throughput are performed in Section IV. Numerical results are presented in Section V. The concluding remark is given in Section VI.

II. Pulse-level Beam Switching: Physical Layer Envision

In this section, we further motivate TRPLE and describe the expected physical layer and the transceiver structure. To our knowledge, the implications of pulse-level beam-switching on the upper layer protocols have not been investigated. Also, we note that multi-band carrier-modulation is theoretically possible, but impractical due to nonexistence of a supportive digital processor.

Impulse radio with TS-OOK: we assume an impulse radio, which generates pulses which are extremely narrow in time, as demonstrated in [13] [14]. The modulation considered is Time-spread On-off-keying (TS-OOK) [16], which can be supported by current technology. In TS-OOK, the logical "1" is encoded with a pulse, and the logical "0" is encoded with silence. As the channel is frequency-selective (even without multi-path) due to molecular absorption, the gap between consecutive pulses to the same user must be adequately large to tolerate pulse-broadening by the channel, so that equalization is not needed.

Narrow beamwidth: in light of graphene-based nano-antennas [12], we assume that all the THz radios are equipped with electronically steerable antenna arrays. Therefore, directivity can be achieved at both the transmitter and the receiver. With high directivity, transmission-beam is narrow enough to illuminate only one user path, making negligible interference on other users and thus rendering a "pseudo-wired" abstraction of the wireless links [17].

User multiplexing: in an indoor picocell that has one access point (AP) and a number of users, it is assumed that the AP can multiplex users in fast time by illuminating beams to users one at a time, as in Fig.2. Recently, the concept and analysis of beamscanning capability of graphene-based antannas at THz have been presented [15], which however did not specify the scanning frequency. Following the notably property that graphene conductivity can be easily tuned by electric field effect [15] [18], taking one step further we reasonably envision that in all-graphene devices beams can be switched at nearly pulse-level with sufficiently small switching time.

Energy control: in THz Band, the transceiver has limited capabilities in power control and coherent detection. Thus, we assume all pulses have the same power. Further, we assume transmitter pulse shaping is not practical because of too much overhead and channel state information (CSI) aging is severe due to poor transmitter self-coherence. It is also assumed that receiver equalization is not practical because signal processing takes too much time compared with the time scale of Terahertz signal. Coherent receivers require correlators, suffering from burden of channel estimation for large antenna arrays and synchronization errors. Because of these assumptions, we consider an energy detection (ED) receiver that collects energy from the pulses. Thus, the AP controls the transmission-energy by modulating the number of repeated pulses to users.

III. THz Pulse-level beam-switching with energy control (TRPLE)

In this section, we describe the principles of the proposed THz Pulse-level Beam-switching with Energy control (TRPLE), designed upon the emitter and detector as discussed in Section II. We consider a typical indoor picocell, where the access point (AP) communicates with a group of users. In addition to line-of-sight (LOS) transmission whenever possible, the presence of blockage foresees directed non-LOS (NLOS) transmission [3]. In this context, we present the MAC protocol to solve three problems: (1) neighbor discovery, (2) transmission scheduling, and (3) energy control.

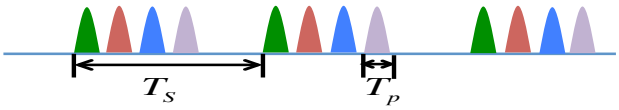

Figure 2: llustration of pulse-level beam-switching.

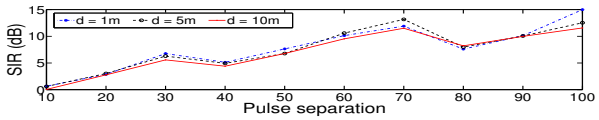

Figure 3: Signal to inter-symbol interference ratio v.s. Pulse separation (in terms of number of pulse length)

A. Pulse-level Beamscanning Neighbor Discovery

The purpose of neighbor discovery in TeraNets is to identify users along with the best beam direction to reach them. The best direction should be along the direct path in the LOS case and the strongest path in the NLOS case. Similar to [17] [19], we assume that nodes are placed on a two-dimensional plane, and we do not consider variation in the beam pattern over the elevation angle. We expect that typically communication does not occur over the whole sphere, and infrequent activities can be solved by certain localization schemes.

Following a spatial scan-based approach, the AP points the thin beam rotationally into all possible directions. Existing works for narrow-band systems require the beam to dwell in one direction sending an entire packet and waiting for the acknowledgment, before being able to steer to another direction, incurring substantial delay. In contrast, ultrashort-pulse modulation in THz opens the door to pulse-level beam-switching, in which scanning is interleaved in pulse. Fig.2 depicts the scanning process, where different beam directions are illuminated by beams of different colors. The key benefit is the abilities to scan all directions in one packet time, thanks to the interleaved pulses destined to different directions.

We note that there is a minimum requirement on the pulse separation for the same direction (user), T_s, as in Fig.2. Firstly, the pulse separation T_s must be larger than the delay spread (DS) of the channel. The DS is a function of both multipath DS and DS caused by molecular absorption. With the considered narrow beamforming, the multipath part is quite diminished. The pulse separation must be long enough to allow pulse broadening to die off at the target user before the next pulse arrives. One-hundred-femtosecond-long first-order derivative of Gaussian pulse is assumed. Fig.3 shows the signal to inter-symbol interference ratio (SIR) varied over different pulse separations in terms of the number of pulse length, where the inter-symbol interference accounts for 120 precursor pulses and 120 postcursor pulses. The SIR increases as the pulse separation increases, and exceeds 10 dB for all distances from 1 m to 10 m, when the pulse separation is 100 times of pulse length. Thus, with a safe margin we assume $T_s = 100T_p = 10$ picoseconds. Further, we validate T_s by looking at the total number of directions. Assuming 5^o degree beam-width, minimum 72 beams are required to cover all possible directions, and this number is less than 100 - the maximum number of pulses within T_s.

During scanning, users acquire the best beam towards them. In next packet time, users feedback to the AP using a thin beam in the same interleaved fashion as in the AP scanning phase, For each user, the start time of sending its first pulse is according to the beam index corresponding to the direction it receives from. After feedback, the AP builds an occupancy cache table in its own memory, which is one-to-one mapping of user's ID and its beam direction. Since it is not necessary that all directions are occupied, the AP then allocates transmission sequence for the users, which will synchronize to their allocated time slot.

B. Transmission Scheduling and Energy Control

In THz networks, MAC protocols mainly focus on "scheduling," as opposed to conventional "fighting for access." Tailored to the pulse generator and energy detection receiver, our MAC also performs "energy control" by deciding the number of pulses needed to reach the users. Note that a receiver at far distance may need to collect energy from more than one pulse to decode a bit "1." The notable difference of TRPLE-based data transmission is that packets for different users are interleaved in pulse, as opposed to concatenated packet transmission in conventional directional schemes. The multiplexing benefit is the same as discussed in Subsection A.

1) Energy Control: In the downlink (DL), to guarantee a certain received single-to-noise ratio (SNR), the AP controls the transmission energy by modulating the number of repeated pulses N, which is user dependent. In particular, N depends on the transmit-receiver (TR) separation d, LOS or NLOS path, total path length r, and angle of incidence ψ, i.e., $N = func\{d, \text{LOS/NLOS}^1, r, \psi\}$. More details will be presented in Section IV. Similar arguments apply to the uplink (UL) transmission, where users control the number of pulses sent to the AP.

2) Frame Structure: As in Fig.4, a MAC frame is composed of a POLL period, a DL period and a UL period. During the POLL period, the AP learns the traffic demand of the users and then schedules the DL and UL transmissions. As an illustrative example in Fig.4, all the three users have DL demand, while only User 2 and User 3 have UL demand; the far user (User 1) requires 4 pulses to decode "1," while the middle user (User 2) and the near user (User 3) require 2 and 1 pulses to decode "1," respectively. In this particular example, the data rate ratio among the three users is $1:2:4$. We present general analyses for the data rates in next section.

IV. Stochastic Analysis of TRPLE

In this section, we present stochastic analyses to quantify the data rate of an arbitrary user and the network throughput achievable under TRPLE. In this paper, we focus on the downlink analysis.

[1]Whether a path is LOS or NLOS can be practically learned by, among others, the polarization diversity approach [20].

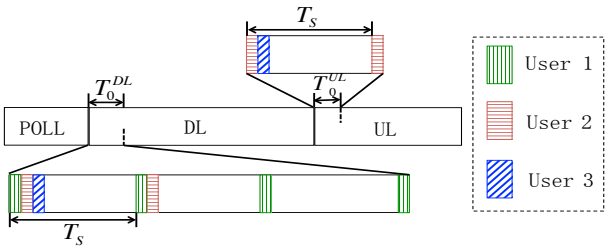

Figure 4: MAC frame structure.

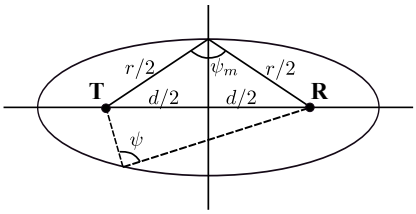

Figure 5: Illustration of angle of incidence, given d and r.

We assume that the transmitter generates a Gaussian pulse [16], which can be expressed as

$$p(t) = \frac{A_0}{\sqrt{2\pi}\sigma} e^{-(t-t_0)^2/(2\sigma^2)}. \quad (1)$$

The power spectrum density (PSD) of the n-th[2] derivative of a Gaussian pulse is given by

$$S^{(n)}(f) = A_0^2 (2\pi f)^{2n} e^{-(2\pi\sigma f)^2}. \quad (2)$$

A. LOS/NLOS Channel Model

We first present our channel model. Extending the LOS model in [7], we consider both LOS and NLOS. The PSD of the channel is given by

$$|H(f,\psi,r)|^2 = \left(\frac{c}{4\pi f r}\right)^2 e^{-k(f)r} L(f,\psi), \quad (3)$$

where the term $\left(\frac{c}{4\pi f r}\right)^2$ is the spreading loss, c is the speed of light, f is the frequency, r is the total path length, $e^{-k(f)r}$ is the molecular absorption loss [3] originated from the excitation of molecular by EM waves at specific frequency computed by the Beer-Lamber Law, and, $L(f,\psi)$ is the rough surface reflection loss that characterizes the loss in the case of NLOS, and is expressed as

$$L(f,\psi) = \begin{cases} \rho_{rough}^2(f,\psi) & \text{if NLOS,} \\ 1 & \text{if LOS.} \end{cases} \quad (4)$$

$\rho_{rough}(f,\psi)$ is reflection coefficient, which depends on the frequency f and the angle of incidence ψ. According to Kirchhoff theory, the reflection coefficient of a rough surface can be obtained as the product of the smooth surface reflection and the Rayleigh roughness factor, as follows

$$\rho_{rough}(f,\psi) = \rho_{smooth} \exp\left[-2\left(2\pi \frac{f}{c}\sigma_h \sin\psi\right)^2\right], \quad (5)$$

where, ρ_{smooth} is the reflection coefficient if the surface were smooth, σ_h is the standard deviation of the height distribution, and, ψ is the angle of incidence.

Without loss of generality, consider the Transverse Electric (TE) part of the EM wave, the smooth surface reflection coefficient is derived from the Fresnel equations:

$$\rho_{smooth} = \frac{\cos\psi - \sqrt{n_t^2 - \sin(\psi)}}{\cos\psi + \sqrt{n_t^2 - \sin(\psi)}}, \quad (6)$$

where n_t is the refractive index. In this paper, we use the measured results $\sigma_h = 0.05$e-3 and $n_t = 1.922 + 0.057j$ [21].

B. Energy Modulation and Conditional Data Rate

We then determine the number of pulses that a given user of total path length r requires to successfully detect the symbol. First, the received signal power of a single pulse is given by

$$P_0(r,\psi) = \int_B S^{(1)}(f) \left(\frac{c}{4\pi f r}\right)^2 e^{-k(f)r} L(f,\psi)\,\mathrm{d}f. \quad (7)$$

Then, accounting for the antenna array gain, G_T and G_R, the received signal power of total N_p pulses is given by

$$P(r,\psi) = N_p G_T G_R P_0(r,\psi). \quad (8)$$

On the other hand, the noise power is obtained as

$$W(r) = \int_B N_o(f,r)\mathrm{d}f = k_B \int_B T_{noise}\,\mathrm{d}f, \quad (9)$$

where k_B stands for Boltzmann constant, and T_{noise} refers to the equivalent noise temperature.

Hence, the minimum number of pulses to guarantee an decoding threshold θ is determined as

$$N_p(r,\psi) = \min_n\{n : \frac{P(r)}{W(r)} \geq \theta\} \quad (10)$$

$$= \left\lceil \frac{\theta K_B \int_B T_{noise}\,\mathrm{d}f}{G_{tx}G_{rx}\int_B S^{(1)}(f,r)(\frac{c}{4\pi f r})^2 e^{-k(f)r} L(f,\psi)\,\mathrm{d}f} \right\rceil. \quad (11)$$

Accordingly, the maximum data rate conditioned on the total path length r and angle of incidence [4] ψ, is obtained as

$$\Upsilon(r,\psi) = \frac{1}{T_s N_p(r,\psi)}. \quad (12)$$

C. Data Rate of An Arbitrary User

We now consider the data rate conditioned on T-R separation d. In the LOS case, $r = d$. In the NLOS case ($r > d$), the propagation time τ_i of the NLOS path is larger than the LOS propagation time τ_0, which equals to d/c. We can introduce a maximum path delay, τ_m such that $\tau_0 \leq \tau_i < \tau_m$, and assume

[2]The first derivative is used in this paper.

[3]Detailed calculation of $k(f)$ can be found in [7].

[4]in the case of LOS, ψ is NULL.

that reflectors are uniformly distributed in space. Conditioned on the T-R separation d, the probability distribution function (PDF) of the normalized total path delay τ, i.e., sum of the incident path and the reflected path, is given by [22]

$$f_{\hat{\tau}}(\hat{\tau}|d) = \frac{2\hat{\tau}^2 - 1}{\beta\sqrt{\hat{\tau}^2 - 1}}, \quad 1 \leq \hat{\tau} < \hat{\tau}_m, \tag{13}$$

where $\beta = \hat{\tau}_m\sqrt{\hat{\tau}_m^2 - 1}$, and $\hat{\tau}_m = \tau_m/\tau_0 = \tau_m c/d$. The total path length r is linearly proportional to $\hat{\tau}$, $r = \hat{\tau}d$. Therefore, the PDF of the total path length is obtained as

$$f_r(r|d) = \frac{2(r/d)^2 - 1}{d\beta\sqrt{(r/d)^2 - 1}}, \quad d \leq r < \hat{\tau}_m d. \tag{14}$$

We now consider the rate of User i, conditioned on d, by averaging over r and ψ. The conditional mean of the rate is given by

$$\mathbb{E}\left[\Upsilon_i|d\right] = p_0\mathbb{E}\left[\Upsilon_i^{(0)}|d\right] + p_1\mathbb{E}\left[\Upsilon_i^{(1)}|d\right], \tag{15}$$

where, the expectations are taken over r and ψ, the first component represents the case that user i is a LOS user, and, the second component, a NLOS user. p_0 and p_1, which are related to shadowing, are the probabilities of being a LOS or a NLOS user.

In the LOS case, $r = d$. Thus, we have

$$\mathbb{E}\left[\Upsilon_i^{(0)}|d\right] = \Upsilon_i^{(0)}(d). \tag{16}$$

In the NLOS case, we have

$$\mathbb{E}\left[\Upsilon_i^{(1)}|d\right] = \int_d^{\tau_m c} f_r(r|d)\int_0^{\psi_m} f_\psi(\psi|r,d)\Upsilon_i^{(1)}(r,\psi)\,\mathrm{d}\psi\,\mathrm{d}r. \tag{17}$$

We assume that the angle of incidence is uniformly distributed between 0 and the maximum ψ_m, given (d, r), i.e.,

$$f_\psi(\psi|r,d) = \begin{cases} \dfrac{1}{\psi_m} & 0 \leq \psi \leq \psi_m, \\ 0 & \text{otherwise}, \end{cases} \tag{18}$$

where $\psi_m = \arcsin(d/r)$, as illustrated in Fig.5.

Finally, we substitute (16) (17) into (15).

Remark: p_0 and p_1 can be determined by log-normal distribution with a threshold, similar to the shadowing model. Using the cumulative distribution function (CDF) of a log-normal random variable $\ln\mathcal{N}(\mu, \sigma^2)$, we get

$$p_0 = 1 - p_1 = \frac{1}{2}\mathrm{erfc}\left(-\frac{\ln x_0 - u}{\sigma\sqrt{2}}\right), \tag{19}$$

where $\mathrm{erfc}(\cdot)$ is the complementary error function, and x_0 is the threshold determining whether the beam is LOS or NLOS.

D. Throughput of a THz Network

Taking the stochastic geometry approach, we assume that users are distributed according to a Poisson point process (PPP), with intensity λ. Thus, the number of users inside any bounded region $A \in \mathbb{R}^{dim}$, $N(A)$, follows the Poisson distribution

$$\mathbb{P}\left[N(A) = k\right] = \frac{(\lambda A)^k e^{-\lambda A}}{k!}. \tag{20}$$

In a PPP network, consider the ith user, which is ith nearest neighbor to the AP. The distance between User i and the AP (T-R separation) follows the generalized Gamma distribution

$$f_{D_i}(d) = d^{2i-1}(\lambda\pi)^i\frac{2}{\Gamma(i)}e^{(-\lambda\pi d^2)}, \quad d \geq 0. \tag{21}$$

Then, averaging over the distribution of d yields

$$\mathbb{E}\left[\Upsilon_i\right] = \int_0^{d_m} f_{D_i}(d)\mathbb{E}\left[\Upsilon_i|d\right]\,\mathrm{d}d. \tag{22}$$

With some straightforward manipulations, we have

$$\mathbb{E}\left[\Upsilon_i\right] = \int_0^{d_m}(X + YZ)\,\mathrm{d}d, \tag{23}$$

where $X = p_0 f_{D_i}(d)\Upsilon_i^{(0)}(d)$, $Y = \frac{p_1 f_{D_i}(d)}{\tau_m c\sqrt{\tau_m^2 c^2 - d^2}}$, and $Z = \int_d^{\tau_m c}\frac{2r^2 - d^2}{\sqrt{r^2 - d^2}\arcsin(d/r)}\int_0^{\arcsin(d/r)}\Upsilon_i^{(1)}(r,\psi)\,\mathrm{d}\psi\,\mathrm{d}r$.

As the AP performs user multiplexing in the downlink by illuminating beams to users one at a time, the network throughput is the summation of rates of the scheduled users. Finally, the network throughput can be expressed as

$$\Upsilon = \sum_{k=1}^{K}\left\{\mathbb{P}\left[N(A) = k\right]\sum_{i=1}^{k}\mathbb{E}\left[\Upsilon_i\right]\right\}, \tag{24}$$

where K is a sufficiently large number.

V. Numerical Results

In this section, we present numerical results for the achievable data rate of a single arbitrary user. As THz communication relies on directional transmission through a LOS path or a directed NLOS path, we evaluate two types of users separately. The main parameters used in the numerical evaluation are as follows: the pulse length is 100 femto-seconds, the per-pulse energy is 100 femto-joules, the noise power is -75 dBm, the decoding threshold is -10 dB, and the antenna gains are $G_T = G_R = 35$ dB or 40 dB.

Fig.6 shows the data rates of the LOS and NLOS users. In Fig.6(a), the data rates of a LOS user are plotted versus different LOS distances d. As the distances increase, the overall path loss surges and thus the data rates show a decreasing trend. The curve is not smooth because of the ceiling operator in Eq.(11). Specifically, at $1\text{ m} < d < 7\text{ m}$, the data rate is 0.1 Tbps $= 10^{11}$ bps, while the data rates reduce sharply to 0.05 Tbps, 0.05 Tbps and 0.035 Tbps for distances of 8 m, 9 m and 10 m, respectively. The rate is constant at 0.1 Tbps at near distances(1-7 m) because the strongly frequency selective channel requires a minimum separation of consecutive pulses to the same user, and also because pulse-based modulation has maximum 1bit/symbol. Although theoretically, more advanced modulation (such as MQAM) may increase the date rate on an order of magnitude, compact THz radios that support those modulation are not foreseen to exist in the very near future.

Fig.6(b) shows the data rates of NLOS users as a function of total path length r and the angle of incidence (AOI) ψ, with antenna gain (AG) of 35 dB. The rates dwindle with increased distance, and depend on the AOI. Under the same

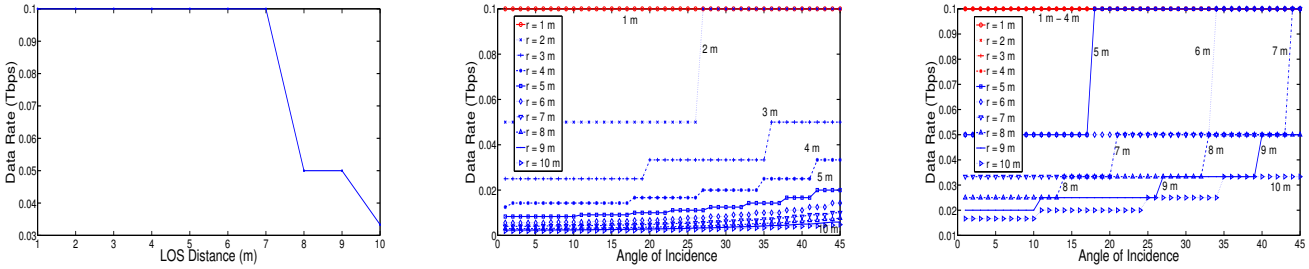

(a) LOS user (antenna gain = 35 dB). (b) NLOS user (antenna gain = 35 dB). (c) NLOS user (antenna gain = 40 dB).

Figure 6: Data rates of LOS and NLOS users.

path length r, larger AOIs incur less reflection loss and thus allow higher rates. Also, it is observed that the rates are less sensitive to AOIs as the distance increases. Specifically, with 35 dB AG, only users at 1 m and nearer can support the rate of 0.1 Tbps. Among other methods, using larger AG to increase rates is more practical than increasing pulse power, considering Graphene-based compact large antenna arrays. Comparing Fig.6(b)(c), with 5 dB increase in AG, even the users at 10 m can support 0.017 Tbps up to 0.033 Tbps. Meanwhile, the users nearer than 4 m can always achieve 0.1 Tbps regardless of the AOI. Again, the non-smoothness of the curves in Fig.6(b)(c) is due to the ceiling operator in Eq.(11).

VI. Conclusions

We present the first MAC protocol (TRPLE) to enable "macro-scale" communication in Terahertz networks. Tailored to THz channel and the expected capability of THz radios, TRPLE utilizes "pulse-level" beam-switching of compact large Graphene-antenna arrays to perform transmission through either line-of-sight (LOS) path or directed NLOS path. In light of "pseudo-wired" THz wireless link, TRPLE solves neighbor discovery and transmission scheduling with fast interleaved pulse beams, and controls the transmission-energy according to users' locations. For the downlink, analytical study is presented to evaluate the achievable data rates of an arbitrary user as well as the network throughput. We found that the minimum pulse separation at the receiver limits the single-user data rate to 0.1 Tbps (100 Gbps), which is fundamentally limited by the molecular absorption of THz channel. Analyses for the uplink will be addressed in the future work.

References

[1] S. Cherry, "Edholm's law of bandwidth," *Spectrum, IEEE*, vol. 41, no. 7, pp. 58–60, 2004.

[2] M. Koch, "Terahertz communications: A 2020 vision," in *Terahertz Frequency Detection and Identification of Materials and Objects*, ser. NATO Science for Peace and Security Series. Springer Netherlands, 2007, pp. 325–338.

[3] R. Piesiewicz, T. Kleine-Ostmann, N. Krumbholz, D. Mittleman, M. Koch, J. Schoebel, and T. Kurner, "Short-range ultra-broadband terahertz communications: Concepts and perspectives," *Antennas and Propagation Magazine, IEEE*, vol. 49, no. 6, pp. 24–39, 2007.

[4] J. Federici and L. Moeller, "Review of terahertz and subterahertz wireless communications," *Journal of Applied Physics*, vol. 107, no. 11, pp. 111 101–111 101–22, 2010.

[5] K.-C. Huang and Z. Wang, "Terahertz terabit wireless communication," *Microwave Magazine, IEEE*, vol. 12, no. 4, pp. 108–116, 2011.

[6] I. F. Akyildiz, J. M. Jornet, and M. Pierobon, "Nanonetworks: a new frontier in communications," *Communications of the ACM*, vol. 54, no. 11, pp. 84–89, 2011.

[7] J. Jornet and I. Akyildiz, "Channel modeling and capacity analysis for electromagnetic wireless nanonetworks in the terahertz band," *Wireless Comm., IEEE Trans. on*, vol. 10, no. 10, pp. 3211–3221, 2011.

[8] R. Choudhury, X. Yang, R. Ramanathan, and N. Vaidya, "On designing mac protocols for wireless networks using directional antennas," *Mobile Computing, IEEE Transactions on*, vol. 5, no. 5, pp. 477–491, 2006.

[9] R. Ramanathan, J. Redi, C. Santivanez, D. Wiggins, and S. Polit, "Ad hoc networking with directional antennas: a complete system solution," *IEEE JSAC*, vol. 23, no. 3, pp. 496–506, 2005.

[10] T. Korakis, G. Jakllari, and L. Tassiulas, "Cdr-mac: A protocol for full exploitation of directional antennas in ad hoc wireless networks," *Mobile Computing, IEEE Transactions on*, vol. 7, no. 2, pp. 145–155, 2008.

[11] J. Pujol, J. Jornet, and J. Pareta, "Phlame: A physical layer aware mac protocol for electromagnetic nanonetworks," in *INFOCOM Workshops*, 2011, pp. 431–436.

[12] M. Tamagnone, J. Gomez-Diaz, J. R. Mosig, and J. Perruisseau-Carrier, "Reconfigurable terahertz plasmonic antenna concept using a graphene stack," *Applied Physics Letters*, vol. 101, no. 21, p. 214102, 2012.

[13] W. Knap, F. Teppe, N. Dyakonova, D. Coquillat, and J. Łusakowski, "Plasma wave oscillations in nanometer field effect transistors for terahertz detection and emission," *Journal of Physics: Condensed Matter*, vol. 20, no. 38, p. 384205, 2008.

[14] L. Vicarelli, M. Vitiello, D. Coquillat, A. Lombardo, A. Ferrari, W. Knap, M. Polini, V. Pellegrini, and A. Tredicucci, "Graphene field-effect transistors as room-temperature terahertz detectors," *Nature materials*, vol. 11, no. 10, pp. 865–871, 2012.

[15] M. Esquius-Morote, J. Gomez-Diaz, and J. Perruisseau-Carrier, "Sinusoidally modulated graphene leaky-wave antenna for electronic beam-scanning at thz," *Terahertz Science and Technology, IEEE Transactions on*, vol. 4, no. 1, pp. 116–122, Jan 2014.

[16] J. Jornet and I. Akyildiz, "Information capacity of pulse-based wireless nanosensor networks," in *IEEE SECON*, June 2011, pp. 80–88.

[17] R. Mudumbai, S. Singh, and U. Madhow, "Medium access control for 60 ghz outdoor mesh networks with highly directional links," in *INFOCOM 2009, IEEE*, April 2009, pp. 2871–2875.

[18] Y.-J. Yu, Y. Zhao, S. Ryu, L. E. Brus, K. S. Kim, and P. Kim, "Tuning the graphene work function by electric field effect," *Nano letters*, vol. 9, no. 10, pp. 3430–3434, 2009.

[19] J. Ning, T.-S. Kim, S. V. Krishnamurthy, and C. Cordeiro, "Directional neighbor discovery in 60 ghz indoor wireless networks," *Perform. Eval.*, vol. 68, no. 9, pp. 897–915, Sep. 2011. [Online]. Available: http://dx.doi.org/10.1016/j.peva.2011.03.009

[20] F. Yildirim and H. Liu, "A cross-layer neighbor-discovery algorithm for directional 60-ghz networks," *Vehicular Technology, IEEE Transactions on*, vol. 58, no. 8, pp. 4598–4604, Oct 2009.

[21] R. Piesiewicz, T. Kleine-Ostmann, N. Krumbholz, D. Mittleman, M. Koch, and T. Kurner, "Terahertz characterisation of building materials," *Electronics Letters*, vol. 41, no. 18, pp. 1002–1004, Sept 2005.

[22] J. Liberti and T. Rappaport, "A geometrically based model for line-of-sight multipath radio channels," in *Vehicular Technology Conference*, 1996, pp. 844–848 vol.2.